ENSO Irregularity

The detailed character of this can be seen in a Hovmoller diagram of SST and zonal wind-stress anomalies as seen in Figure 1.

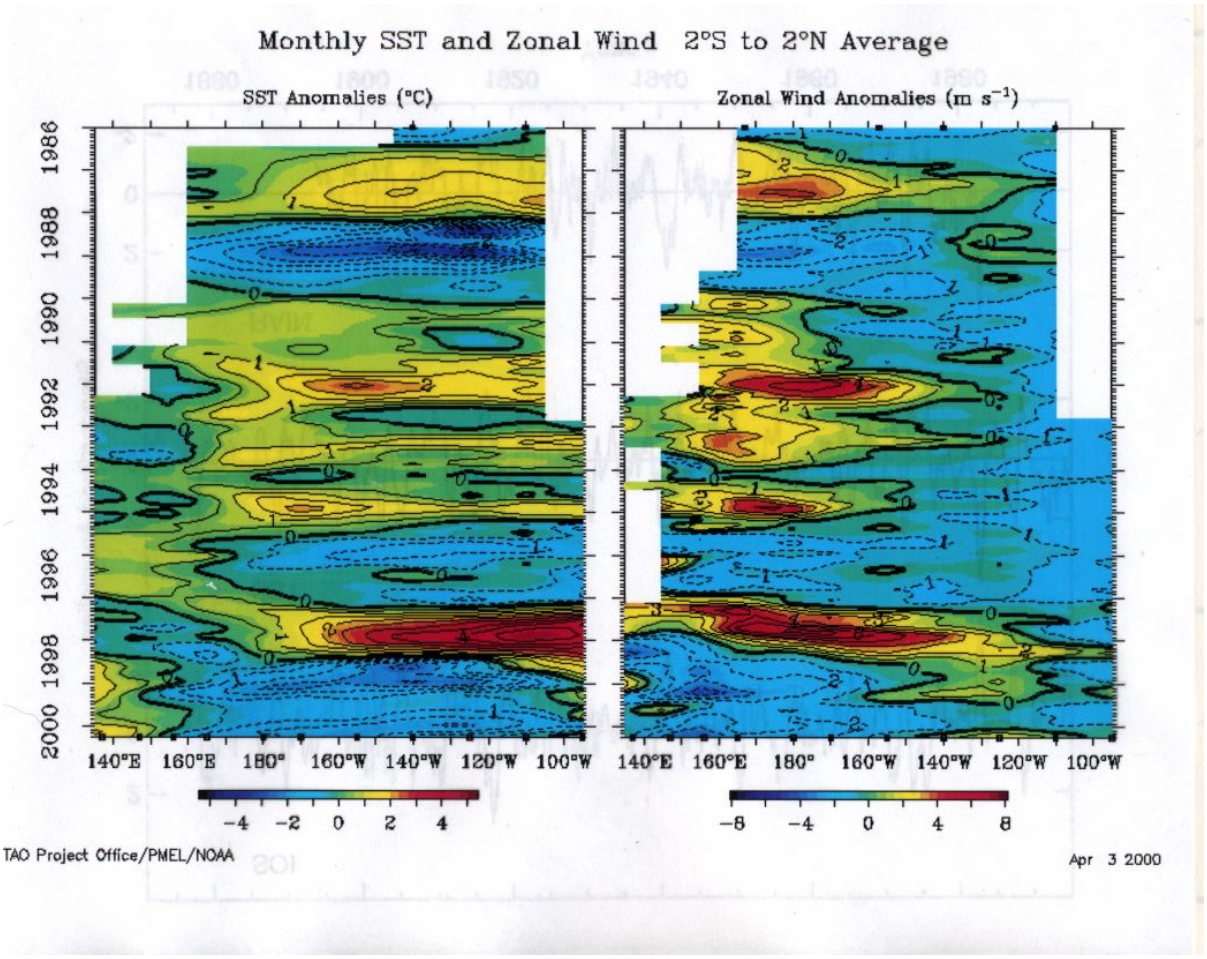

Gross large scale indices of ENSO exist back to the second half of last century. These may

be used to analyze the spectral characteristics of the phenomenon. Depicted in Figure 2 are three independent ENSO indices: The Southern Oscillation Index (SOI), a measure of the zonal gradient in sea level pressure in the tropical Pacific; eastern equatorial SST anomaly and finally central equatorial rainfall anomaly.

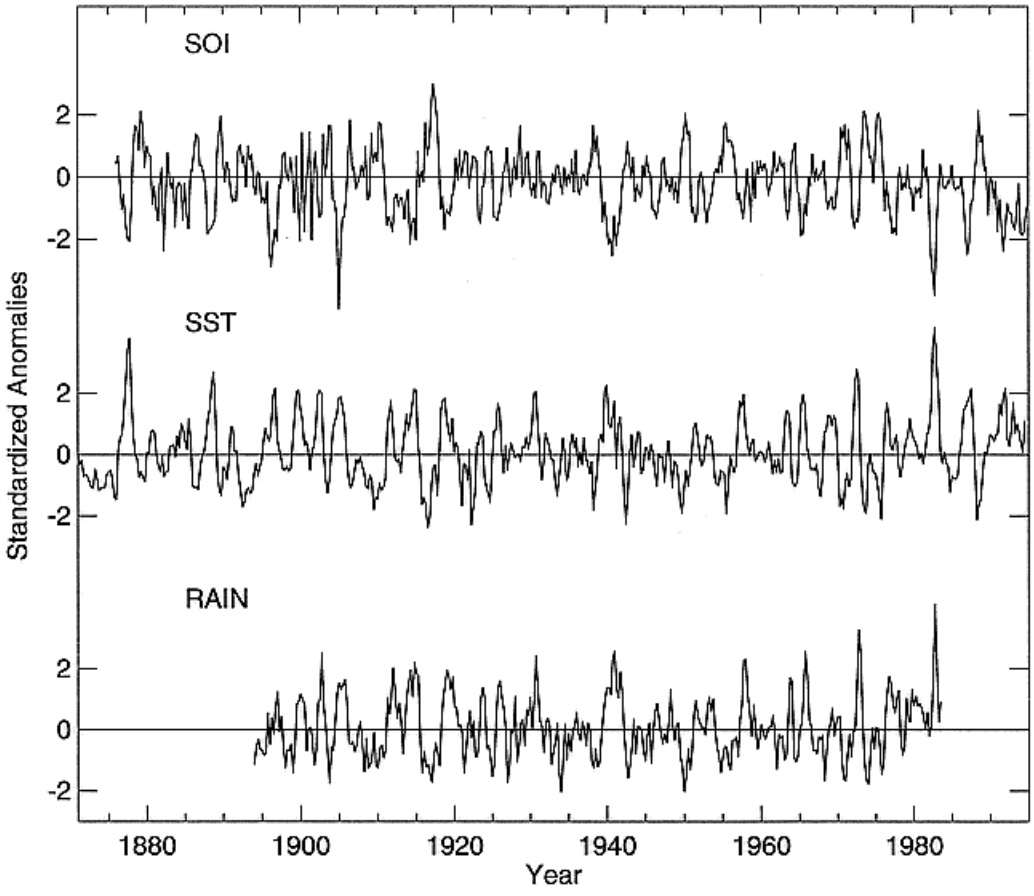

Correlation between these indices shown in Figure 3 are of order $0.6 - 0.8$ and do not vary

greatly between the first and second halves of the record suggesting that they are reliable over the entire period not just the more recent and better observed epoch.

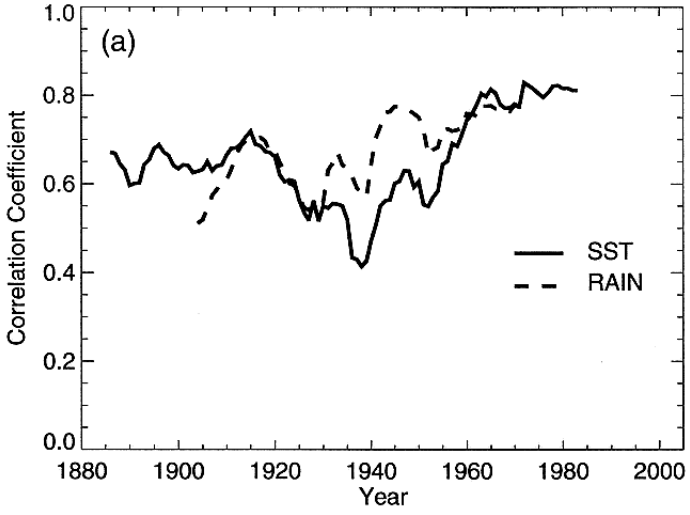

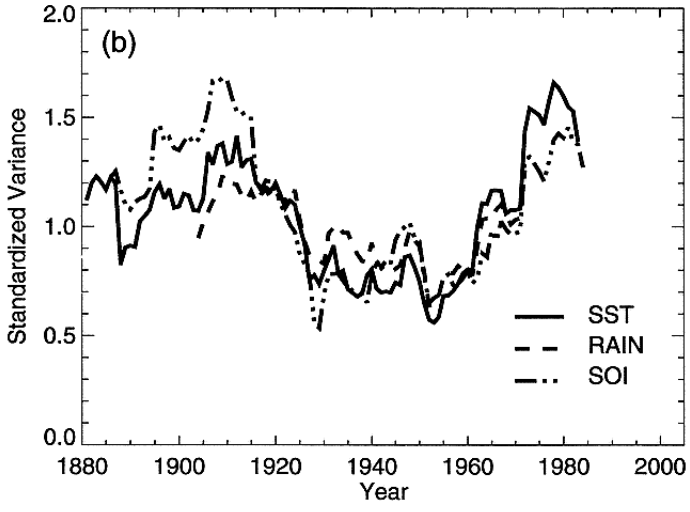

The SST index is somewhat smoother than the

others but clearly displays marked irregularity which any complete theory of ENSO must seek to explain. Notice that there are decades such as the 1980s when strong quasi-periodic oscillations exist while other decades such as the 1930s show a weak quite irregular fluctuation. The spectral density functions for the three indices are displayed in Figure 4 and there is remarkable general agreement. A quite broad peak exists for periods of order 4 years with a marked decline towards higher frequencies which is reminiscent of a red noise process. The robustness of the spectral characteristics is particularly useful from the viewpoint of testing ideas for the mechanism of irregularity.

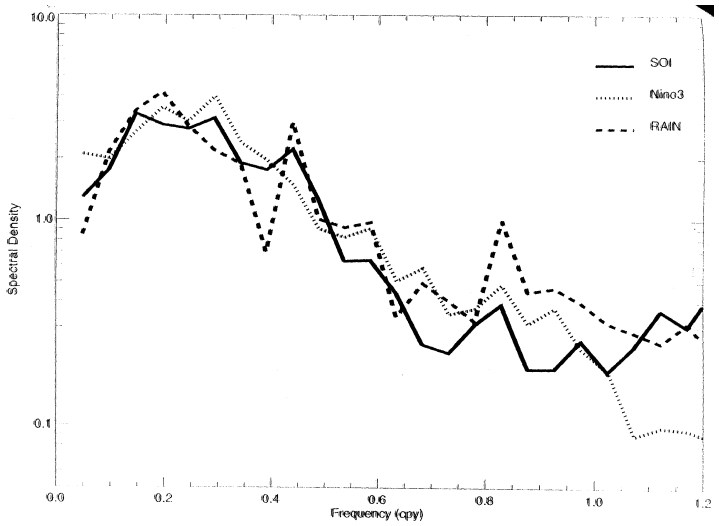

The original success of the Cane and Zebiak model meant that its behavior has been subject to much scrutiny. This model exhibited irregularity whose spectrum bore some resemblance to that of Figure 3. Attempts to reproduce this in other models with a steady state atmosphere (so-called intermediate and hybrid coupled models) proved quite difficult. Neelin in the early 1990s was able to achieve an irregular oscillation which had a chaotic origin. Analysis revealed that the interference between the annual cycle of the model and the delayed action oscillator was responsible for the chaos.

The spectrum of these oscillations however did not show much correspondence with Figure 4 (it had strong spectral peaks at all multiples of the annual cycle) and moreover Neelin demonstrated as seen in Figure 5 that his model needed to be quite selectively tuned to achieve the chaos.

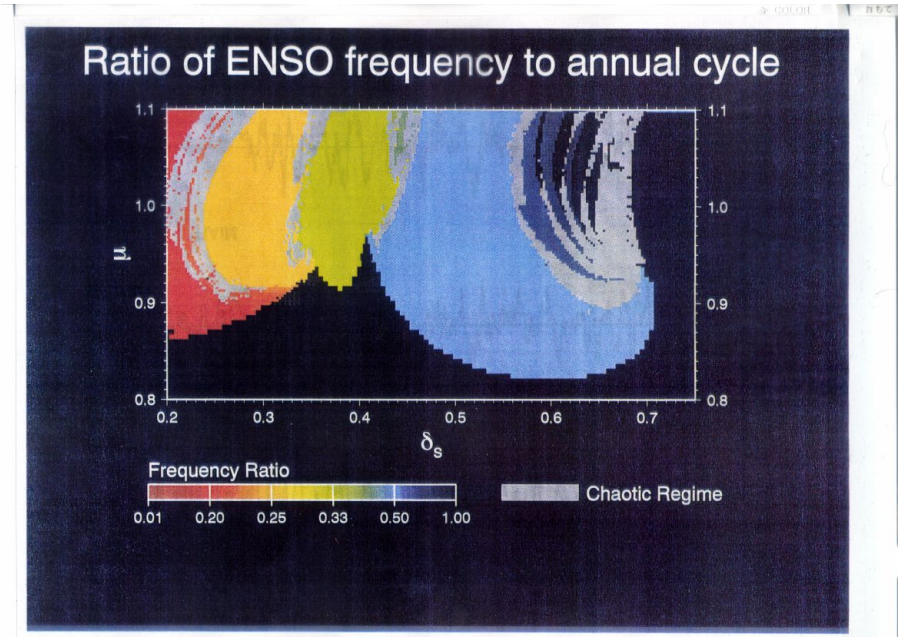

This lack of success motivated myself and a number of others to consider an alternative hypothesis for the irregularity in the early 1990s.

Stochastic Scenario for ENSO Irregularity

An important aspect of atmospheric variability which is absent from intermediate and hybrid coupled models is that generated by internal (primarily non-coupled) instabilities. One important source of such instability is deep moist convection and phenomena such as the MJO and easterly waves result. Other mechanisms such as barotropic and baroclinic instabilities are also undoubtedly responsible for the generation of a large amount of tropical "weather" which is completely unrelated to ENSO. Examination of daily time series of equatorial windstress shows that there is an enormous amount of variability which can at times mask the low frequency changes associated with coupled ocean-atmosphere dynamics. This suggests intuitively that ENSO irregularity may be caused by the effects of these atmospheric transients. Since

the decorrelation time for this variability is of order days it is useful to consider their effects as stochastic forcing of the low frequency coupled climate system. This viewpoint has proved particularly productive in the past ten years and is widely considered a likely cause of ENSO irregularity. Such a view clearly has important implications obviously for ENSO prediction as well since the "stochastic transients" just discussed are unpredictable on climate time scales.

We now outline a mathematical framework for analyzing this scenario. It involves multi-dimensional linear stochastic differential equations (SDEs). Consider a time discretization of a vector SDE

$$u_{\mu+1} = R(\mu+1,\mu)u_\mu + \Delta t f_\mu \qquad (1)$$

where u is a vector in the sense that it may represent spatial variation and also many physical

variables. Time indices are denoted by Greek subscripts. The operator R is the so-called propagator which shifts a state vector forward in time and finally f is a stochastic forcing term whose statistics are assumed to satisfy

$$\begin{aligned} \left\langle f_{j\lambda} \right\rangle &= 0 \\ \left\langle f_{i\mu} f_{j\nu} \right\rangle &= C_{ij}^{\mu\nu} \end{aligned} \tag{2}$$

where we are using Latin subscripts to denote the vector indices. If we iterate equation (1) from some initial time $\mu = 0$ then we obtain

$$u_\mu = R(\mu, 0)u_0 + \Delta t \sum_{\lambda=0}^{\mu-1} R(\mu, \lambda + 1) f_\lambda \tag{3}$$

If we now further assume for simplicity that the noise is white in time (a reasonable assumption for our purposes) then we may write

$$\left\langle f_{i\mu} f_{j\nu} \right\rangle = \frac{1}{\Delta t} \delta_{\mu\nu} C_{ij}$$

From equation (3) we may now easily write down expressions for the first and second moments (mean and covariance) of u_μ

$$\langle u_\mu \rangle = R(\mu, 0) u_0$$
$$\langle u_\mu, u_\mu \rangle = \Delta t \sum_{\lambda=0}^{\mu-1} R(\mu, \lambda+1) C R^*(\mu, \lambda+1)$$

where the star denotes the transpose or adjoint operator. Taking the continuous limit we obtain

$$\langle u(t) \rangle = R(t, 0) u(0)$$
$$\langle u(t), u(t) \rangle = \int_0^t R(t, t^{'}) C R^*(t, t^{'}) dt^{'}$$

Let us now consider the variance with respect to some index (e.g. average eastern equatorial SST)

$$Var(t) = X_{ij} \left\langle u^i(t), u^j(t) \right\rangle$$

where we are assuming the summation convention for repeated latin indices and X_{ij} can be considered the "metric" matrix. It is now easy to show that

$$Var(t) = trace\{ZC\}$$
$$Z \equiv \int_0^t R^*(t,t')XR(t,t')dt'$$

Note that we have completed separated the stochastic forcing represented by the covariance matrix C from the dynamics represented by the operator Z. It is easy to show that both these operators are positive (and hence Hermitian) and therefore have positive eigenvalues. We can therefore write

$$trace\{ZC\} = \sum_{n,m} p_n q_m (P_n, Q_m)^2$$

where the lower case p and q are the eigenvalues of respectively Z and C while the upper

case P and Q are the corresponding eigenvectors. The inner product squared here can be interpreted as vector projection. Thus if the eigenvectors of the noise forcing covariance matrix project onto the dynamical eigenvectors (we call these stochastic optimals) then there will be significant variance (or uncertainty) growth in our index of interest. Obviously if the noise eigenvectors (often called EOFs) resemble the stochastic optimals with largest eigenvalues then maximal variance growth will occur. We have therefore a very convenient framework for analyzing the susceptibility of dynamical systems to disruption by noise.

The spectrum (and eigenvectors) of Z has been evaluated for ENSO intermediate and hybrid models and is always highly peaked with most of the variance growth being caused by the first two eigenvectors (i.e. the p_1 and p_2 values are much greater than the others). These

stochastic optimals are therefore crucial for whether large variance growth can occur. Figure 6 shows the spatial patterns of heat and momentum flux associated with these optimals.

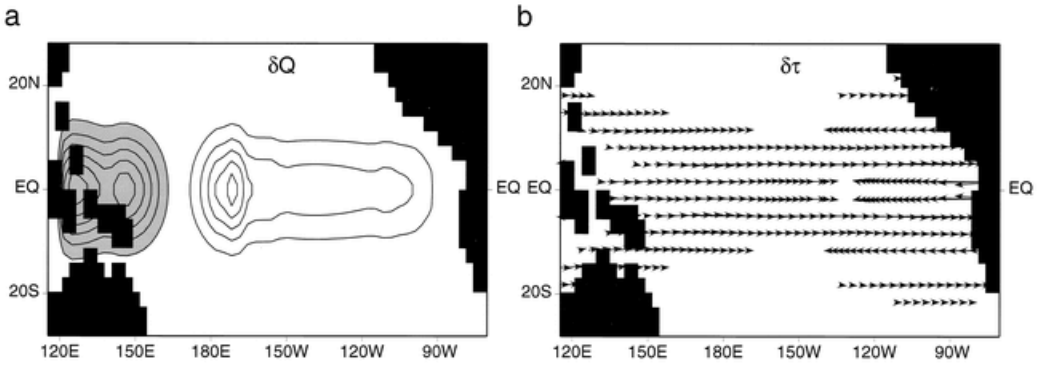

Patterns of forcing such as this within the coupled model quickly grow into SST and wind-stress disturbances resembling the so-called westerly wind burst as is seen in Figure 7:

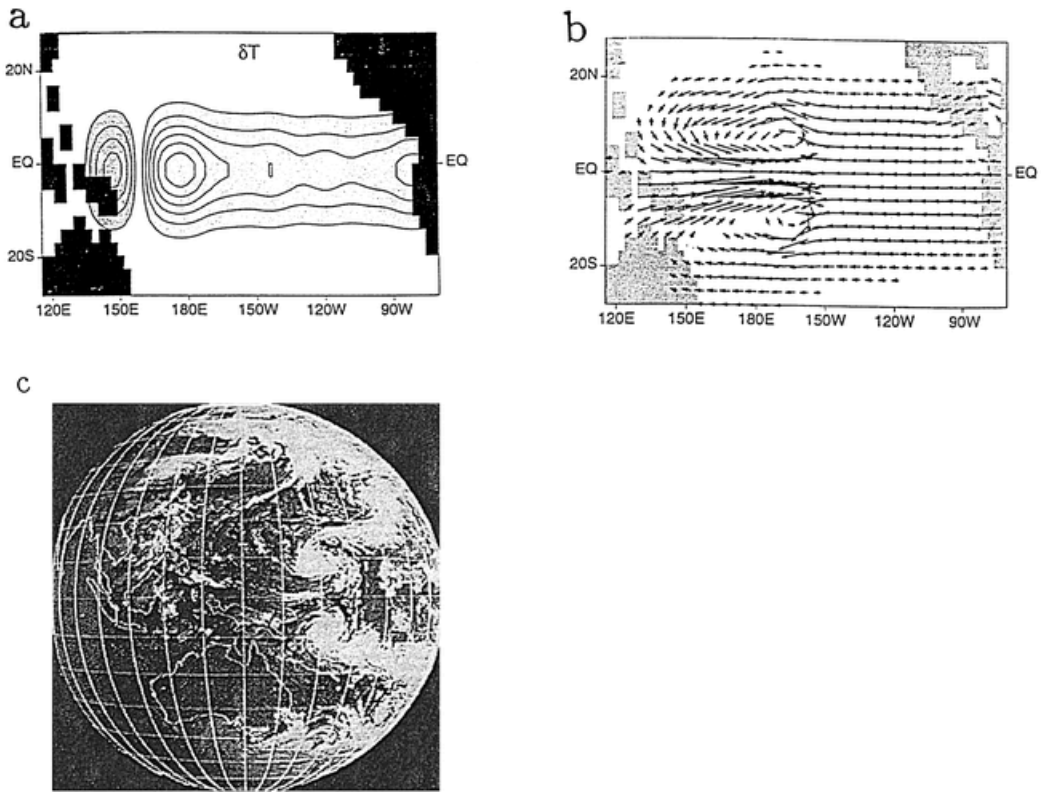

This signature of a disturbance often associated with the Madden Julian Oscillation suggests that this large scale pattern of internal atmospheric variability may be favourably configured to disrupt the ENSO dynamical system. It also says that only noise with large scale spatial coherency will be effective at disruption.

If the ENSO intermediate model above is forced by white noise with the spatial coherency of

the stochastic optimals then an irregular oscillation is induced. Figure 8 shows the result of such forcing on the intermediate coupled model with such noise.

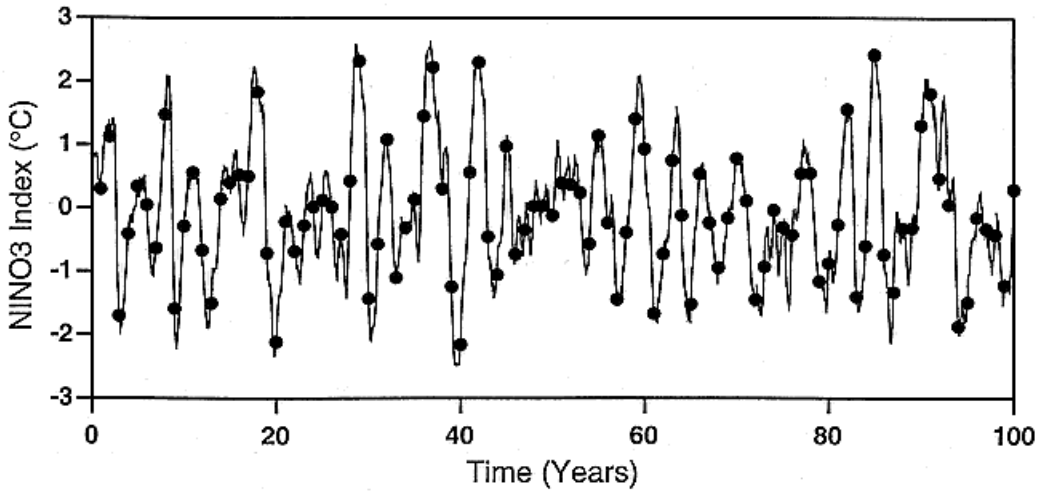

Without the noise a perfectly regular decaying oscillation is observed. The dots show December of each year showing that the observed seasonal synchronization is also achieved. This irregular oscillation shows a clear resemblance to the observed pattern in Figure 2 and the spectrum displayed in Figure 9 is qualitatively the same as the observed spectrum in Figure 4.

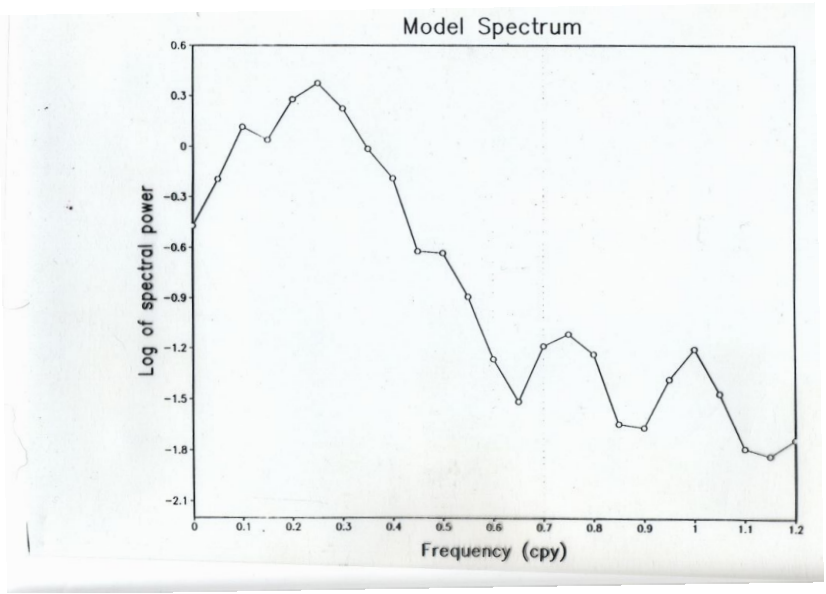

This irregular behavior is particularly robust (one can vary the amplitude of the forcing by some orders of magnitude without effect) and has now been seen by many other investigators using a range of different models. The variance growth curves predicted by this theory are also those observed in physically complete coupled models (CGCMs) which have inbuilt atmospheric transients as part of their atmospheric components.

The implications for predictability of ENSO of this paradigm are also very interesting. It turns

out that the maximal skill to be expected depends on the degree of instability of the low frequency system (i.e. how slowly oscillations without noise decay). The greater the instability the *better* the skill, a rather counter-intuitive result! The consequences for practical predictability are also potentially rather important.

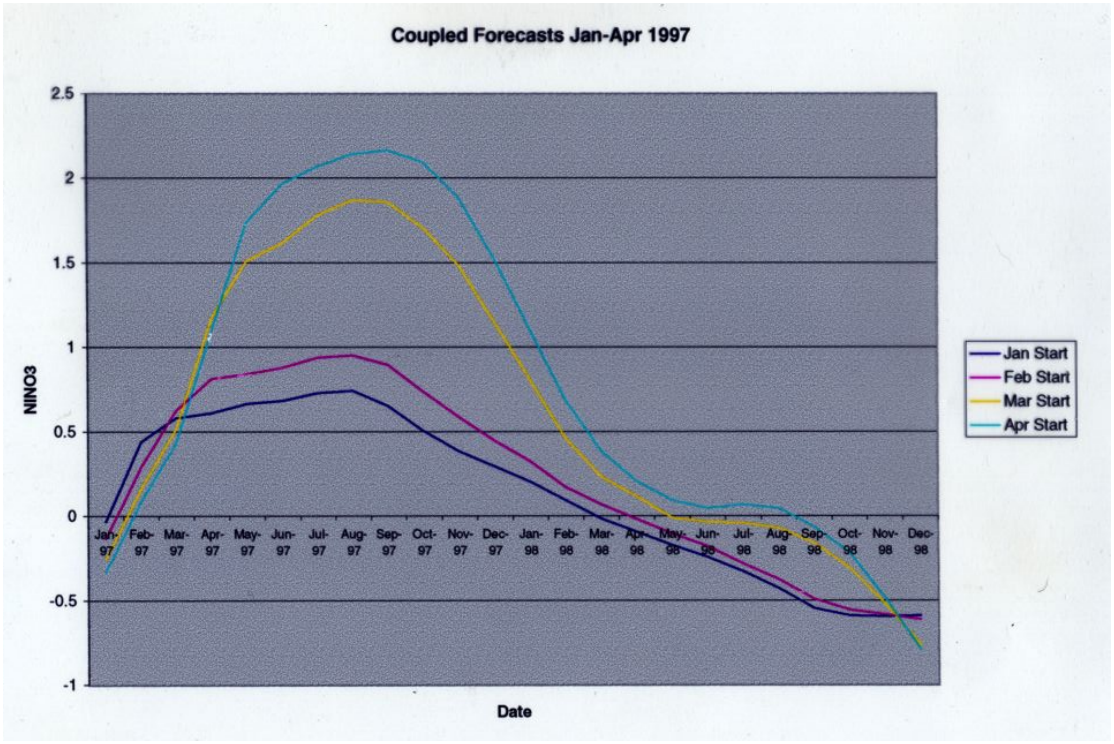

In Figure 10 is a series of forecasts on the 1997-98 monster warm event seperated by one

month. In March a very large westerly wind burst was observed in the western Pacific. This may be the cause of the sharp increase in the magnitude of forecasts.

Some Recent Coupled GCM Results

Such models generally have problems in simulating one of either the mean state; the seasonal cycle or realistic interannual variability. This often makes analysis of the above theoretical ideas problematical. Recently Lengaigne et. al. (Climate Dynamics, 2004) have produced a model which does well on all three counts (Hadley Center AGCM coupled to the LODYC OGCM). Figure 11 shows the performance of the seasonal cycle of SST.

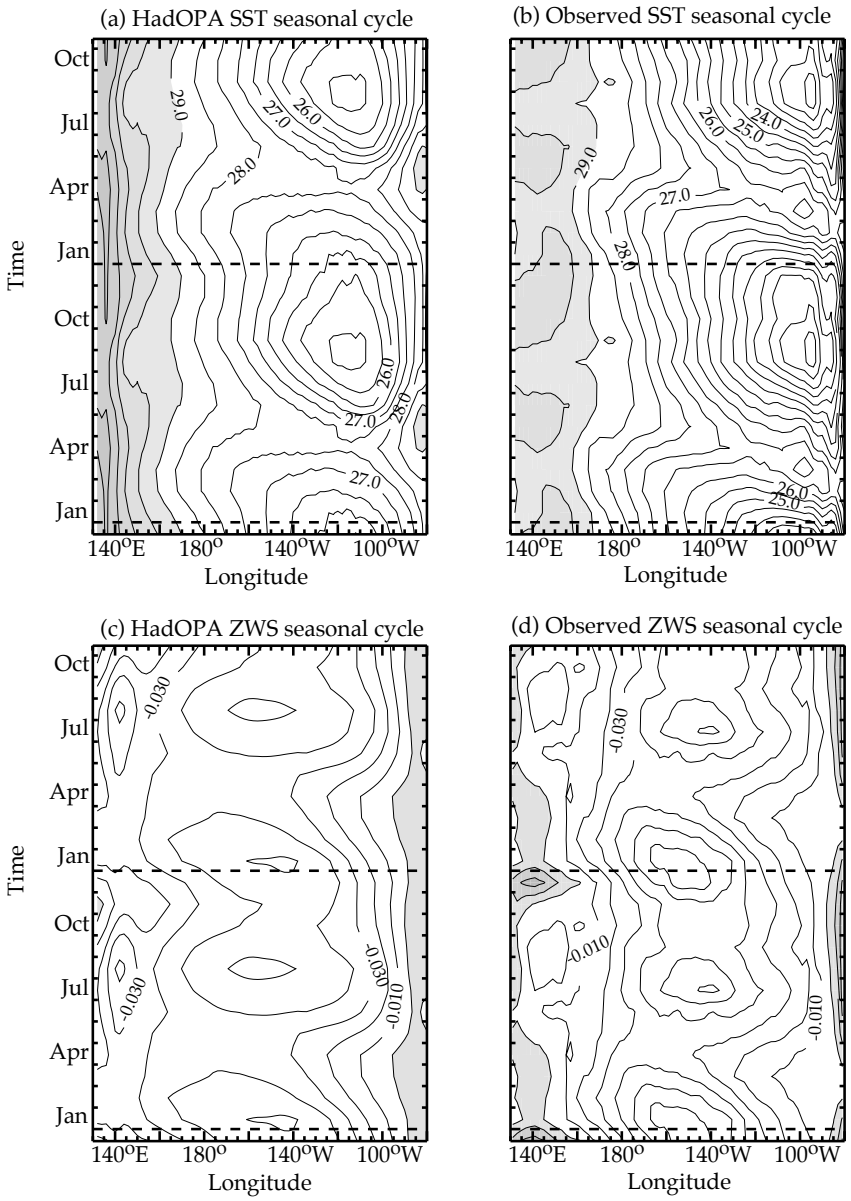
(a) HadOPA SST seasonal cycle
(b) Observed SST seasonal cycle
(c) HadOPA ZWS seasonal cycle
(d) Observed ZWS seasonal cycle
Time
Oct
Jul
Apr
Jan
140°E
180°
140°W
100°W
Longitude
29.0
28.0
27.0
26.0
25.0
24.0
-0.030
-0.010

Figure 4

The interannual variability spectrum is similar to those shown above although somewhat more peaked. The effect of very small perturbations on initial conditions in the model is shown in the upper panel of Figure 12. Shown in the lower panel is what happens if a westerly wind burst is introduced into the model. The perturbation introduced looks like Figure 7 in spatial structure. It's magnitude is similar to that observed in March 1997.

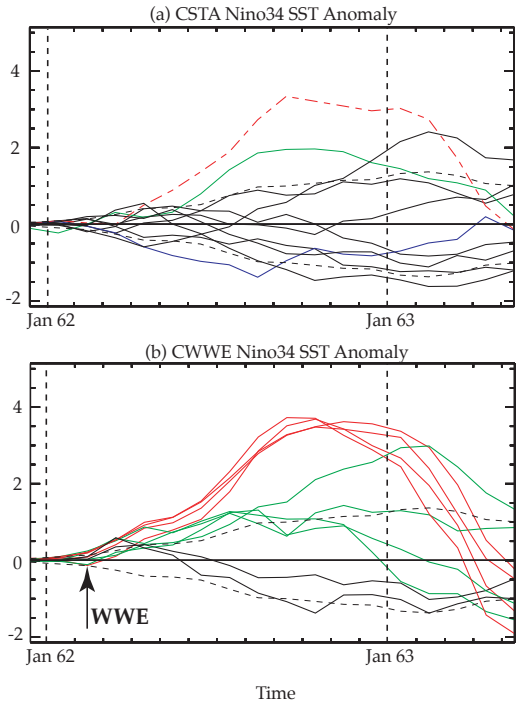

Figure 7

Note the shift in the ensemble towards a strong warm event. The spread of the ensemble with time seen here is also very typical of simple stochastically forced systems.

The strong warm event members of the ensemble look remarkably like the 1997-98 El Nino. Figure 13 shows the model SST and

windstress while Figure 14 shows the observations for 1997-98.

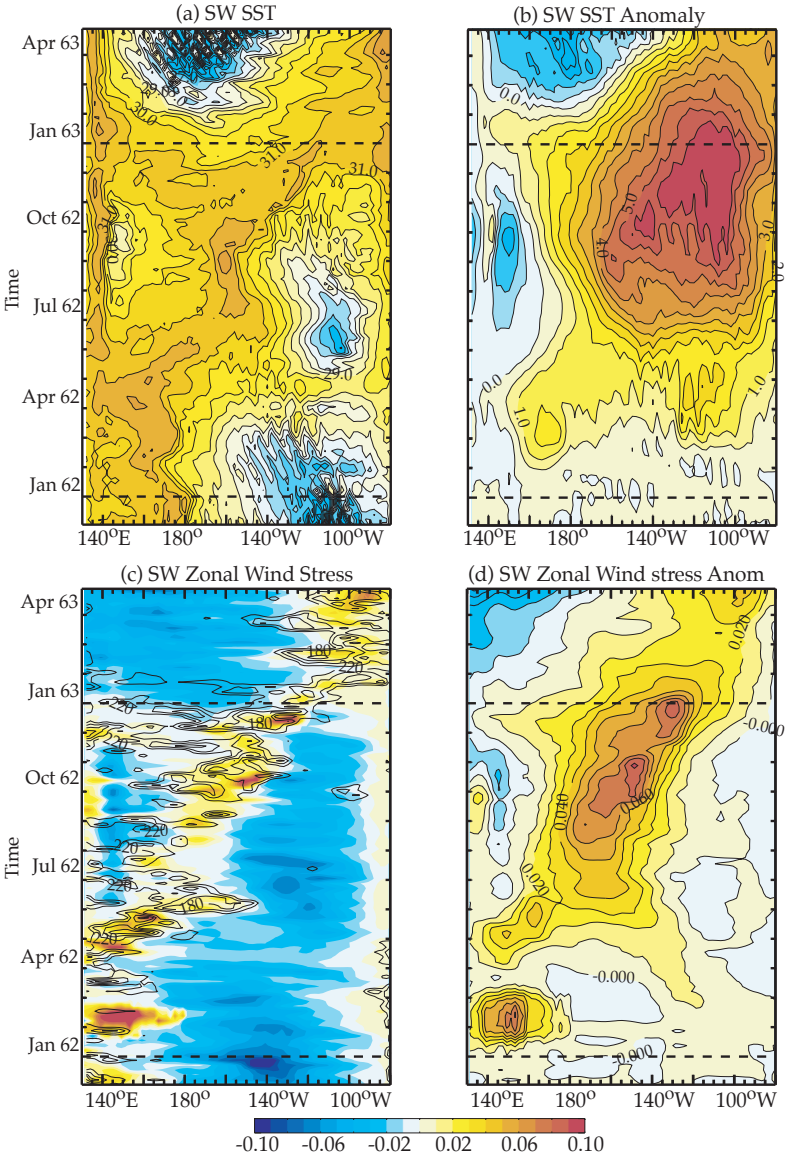

Figure 9

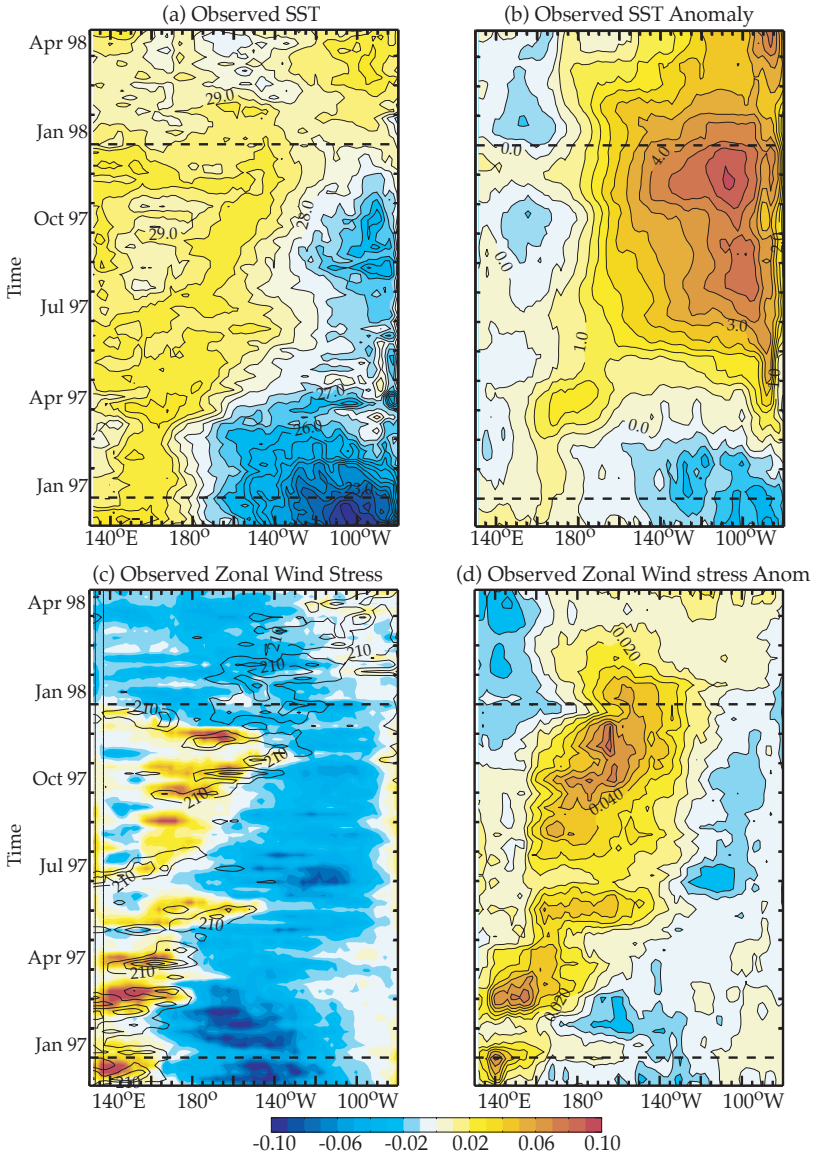

Figure 11

Zonal currents are even remarkably similar as seen in Figure 15.

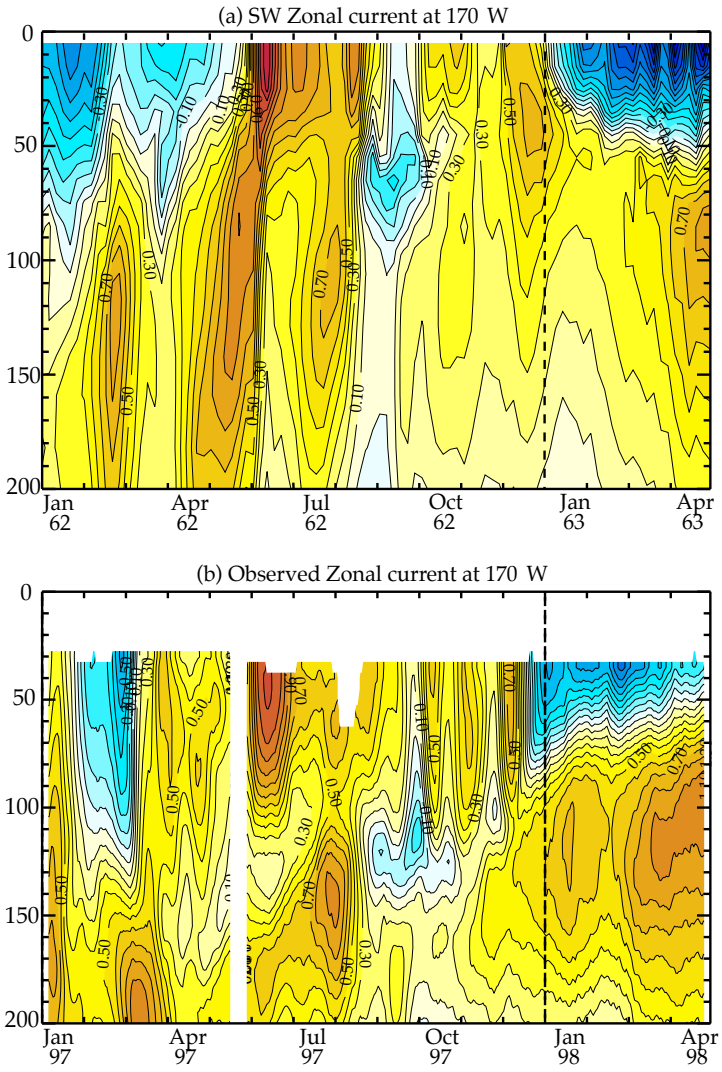
(a) SW Zonal current at 170 W
0
50
100
150
200
Jan 62
Apr 62
Jul 62
Oct 62
Jan 63
Apr 63
(b) Observed Zonal current at 170 W
0
50
100
150
200
Jan 97
Apr 97
Jul 97
Oct 97
Jan 98
Apr 98

Figure 17

Multiplicative Noise?

This issue is only just starting to receive attention in the literature and much work remains. We analyze the issue using the theoretical concepts above. Two things are significant in my view:

1. The stochastic optimals spatial structure and their weighting show considerable variation with the ENSO cycle. In general their weighting is less and more confined to the Western Pacific during cold events and conversely during warm events their weighting is more and the spatial structure is more zonally extended.

2. There is significant evidence that the large scale intraseasonal variability ("MJO") shows

significant variation in zonal extent and amplitude with the ENSO cycle. This is illustrated in a Figure 16 from Kessler (2001):